ESRF	**Experiment title:** **Title:** Structure of Mg- and Zr-based metallic glasses under ultra-high pressure	**Experiment number**: MA-6144
Beamline:	**Date of experiment**: from: 05.04.2024 to: 08.04.2024	**Date of report**: 31.08.2024
Shifts: 9	**Local contact(s)**: MEZOUAR Mohamed	*Received at ESRF:*

Names and affiliations of applicants (* indicates experimentalists):

Lukasz Rogal, Institute of Metallurgy and Materials Science Polish Academy of Science, Reymonta 25 Str. Krakow, Poland

Dominique Laniel Centre for Science at Extreme Conditions and School of Physics and Astronomy, University of Edinburgh, EH9 3FD, Edinburgh, United Kingdom,

Gunnar Weck CEA DAM DIF, Arpajon, France;b Laboratoire Matière en Conditions Extrêmes (LMCE), France

Report:

The proposed project aimed to apply a new thermodynamic path using ultra-high pressure to reach a high-density amorphous (HDA) state of glass-forming Mg- and Zr-based alloys and to study the early-stage crystallization (above T_x temperature) using laser-heated diamond anvil cell experiments. The samples were measured by pair density function measurements (PDF) and X-ray diffraction (XRD). Söller slits were used to enable a better signal-to-noise ratio in the PDF measurements.

Two high-quality metal glasses:

- A $Mg_{61}Cu_{28}Gd_{11}$ %at. glass prepared by melt spinning process (cooling rate of 10 000 K/s) has been loaded into BX90-type DAC and progressively compressed up to a pressure of 50 GPa (Fig. 1a). Neon was used as the pressure transmitting medium (PTM).
- A $Zr_{43}Cu_{43}Al_7Ag_7$ %at. glass prepared by atomization has been loaded into BX90-type DACs and progressively compressed to a pressure of 73 GPa (Fig. 1b). Neon was also used as the PTM.

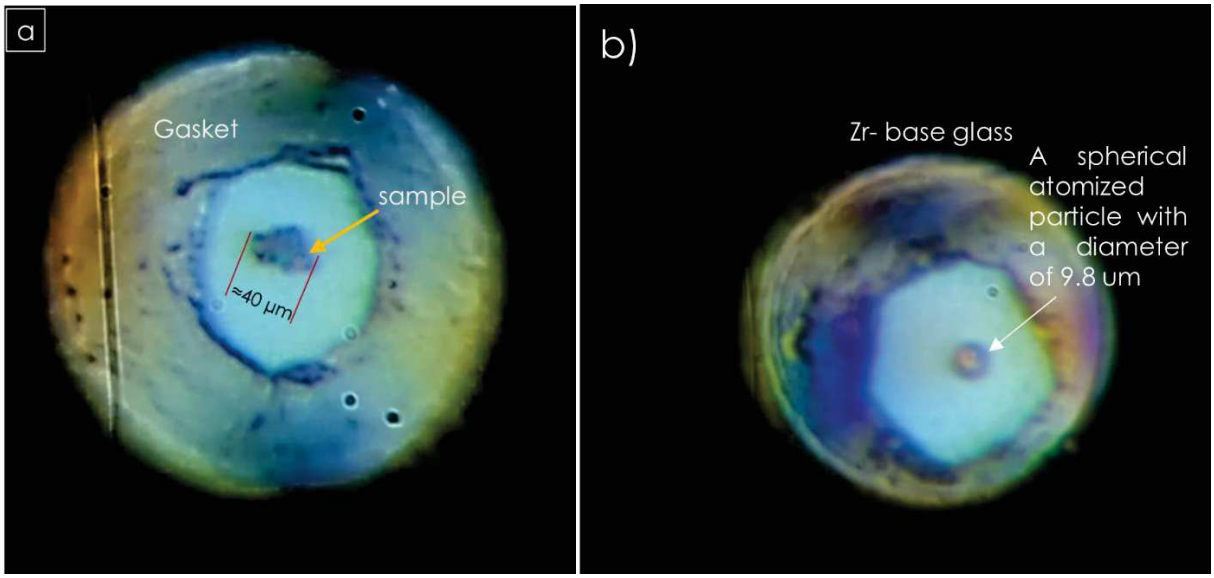

Fig. 1 a) Optical microscopy image of the Mg (a) and Zr (b) glasses in a DAC immediately after gas loading.

I $Mg_{61}Cu_{28}Gd_{11}$ %at. glass

Figure 2 presents structure functions for the alloy $Mg_{61}Cu_{28}Gd_{11}$ %at, comparing a sample compressed up to 50 GPa (black curve) with a sample quenched under pressure after heating above 1500 K (red curve).
When comparing the two curves, a rightward shift of the heated sample is visible, suggesting a reduction in the average atomic distances within the structure, especially in terms of Mg-Mg or Cu-Cu atomic pairs. This shift towards higher **Q** values (~2.98 units) corresponds to a higher-density arrangement of atoms. Typically, in pair distribution function (PDF) analysis, such a shift in **S(Q)** reflects a compression of interatomic distances, as expected under conditions of extreme pressure (50 GPa).
Additionally, the amplitude of the sample after heating is significantly higher, reaching **3.17** units compared to **3.02** for the non-heated compressed sample. The amplitude increase indicates greater atomic ordering or nano-crystallinity in the structure after the heating process. Higher amplitude in **S(Q)** often correlates with improved structural regularity, as atoms settle into a more ordered or crystalline arrangement during cooling under pressure.

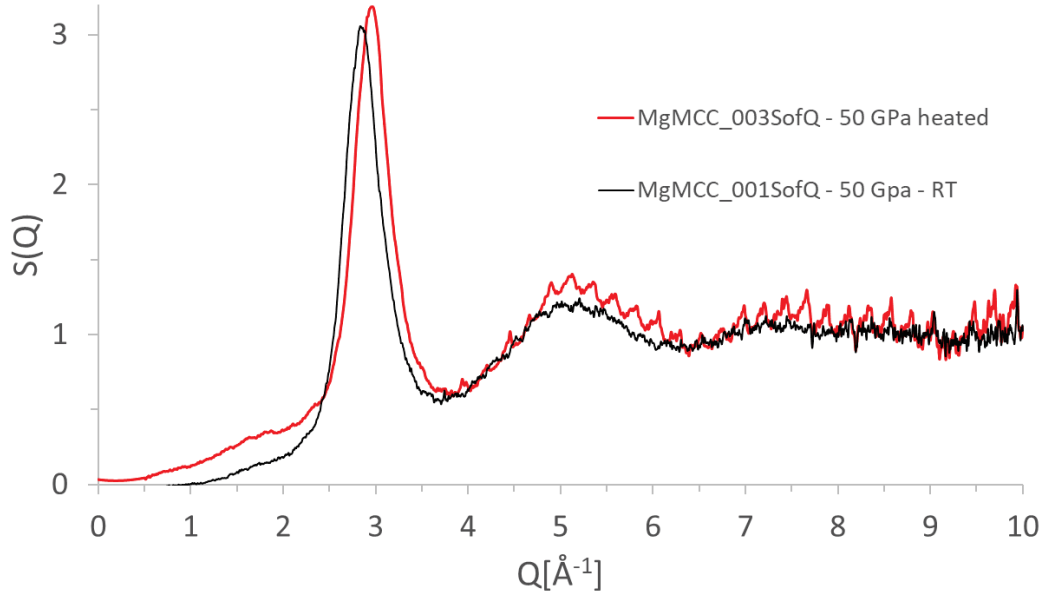

Fig. 2 Structure-function of selected Mg-based glasses.

Figure 3 presents the pair distribution function **G(r)** for the alloy **$Mg_{61}Cu_{28}Gd_{11}$ %at.**, comparing a sample compressed to 50 GPa without heating (black curve) and after heating above 1500 K (red curve).

For the Mg-based glass compressed to 50 GPa without heating, the first harmonic of **G(r)** shows an amplitude of **2.07**, and the peak is positioned at **r ≈ 2.73 Å**. This suggests that the average interatomic distances, particularly for Mg-Mg or Cu-Cu atomic pairs, have shifted due to the high pressure applied. The peak at **2.73 Å** indicates a compressed atomic structure, with bond lengths reduced compared to ambient conditions, where typical Mg-Mg distances range around **3.2–3.4 Å**. The reduced amplitude of **2.07** in the compressed state indicates some degree of structural disorder, where atoms are packed more closely together. The relatively lower amplitude (compared to the heated sample) is be attributed to the amorphous structure.

In contrast, the sample that was both compressed and heated above 1500 K shows a noticeable shift in the peak of **r(A)** to **r ≈ 2.63 Å**. This leftward shift indicates further compression of the atomic distances, which is more pronounced after applying heat. This reduction in the average bond length suggests that heating under pressure allows atoms to rearrange more efficiently, minimizing voids and reducing the average interatomic spacing beyond what compression alone could achieve.
Furthermore, the amplitude of the **G(r)** peak for the heated sample is higher, at **2.36**, compared to **2.07** for the non-heated sample. This increase in amplitude suggests a higher degree of atomic ordering and probably nano-crystallization after the heating process. The elevated temperature likely facilitated atomic diffusion and reorganization, leading to a more uniform and well-ordered structure. The higher amplitude corresponds to a structure with greater regularity in atomic spacing, characteristic of a more crystalline phase or an increased degree of long-range atomic order.

- **Compressed sample (50 GPa, no heating)**: Peak at **r ≈ 2.73 Å**, amplitude of **2.07**. The interatomic distances are compressed, but the structure remains somewhat disordered, likely amorphous or partially crystalline.
- **Heated and compressed sample (50 GPa, >1500 K)**: Peak at **r ≈ 2.63 Å**, amplitude of **2.36**. The leftward shift in the peak suggests further compression of atomic distances, and the increased amplitude indicates greater atomic ordering and crystallinity due to thermal treatment.
- **Comparison**: Heating under pressure leads to a denser, more ordered structure, as evidenced by the higher amplitude and the more compressed interatomic distances compared to the non-heated sample.

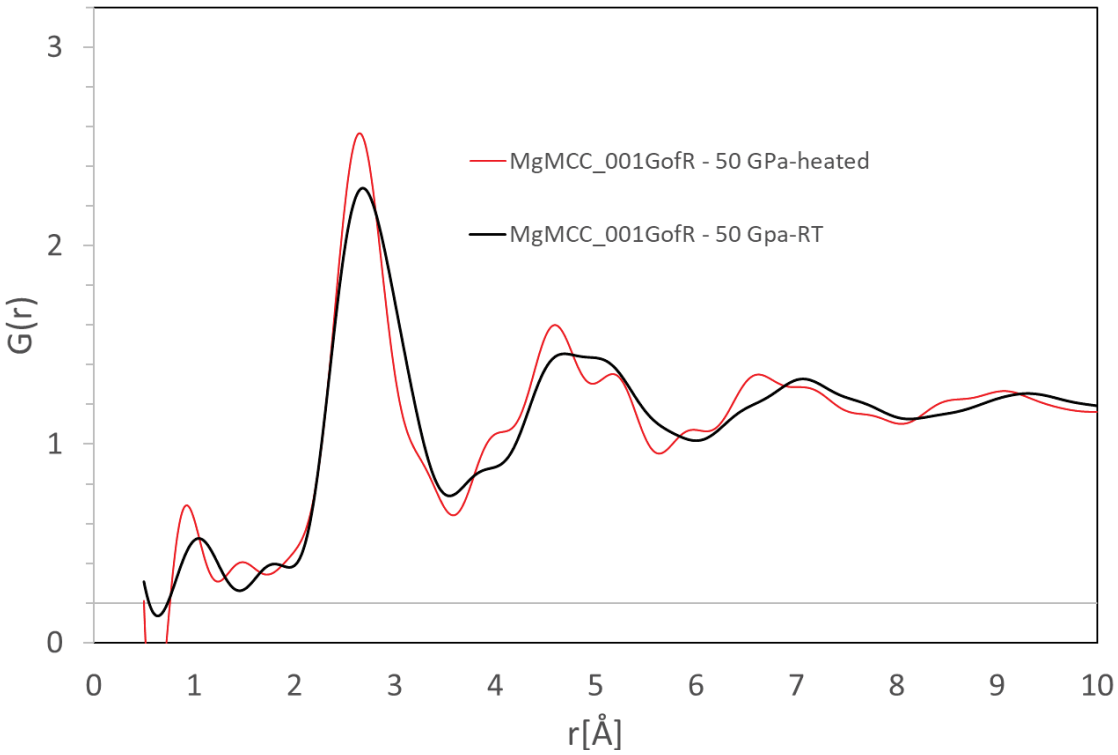

Fig. 3. Reduced pair distribution function corresponding to S(Q) samples shown in Fig. 2.

Additionally, at 50 GPa after heating at the highest temperature, e.g., 2750 K, XRD mapping was conducted (Fig. 4), which evidenced the presence of an amorphous and a crystalline. At this point, the experiments were finished because the crystal structure was obtained. . Next, using a Focussed Ion Beam (FIB), a thin foil of the interphase area (Fig. 5) from the DAC-recovered sample was prepared for TEM studies.

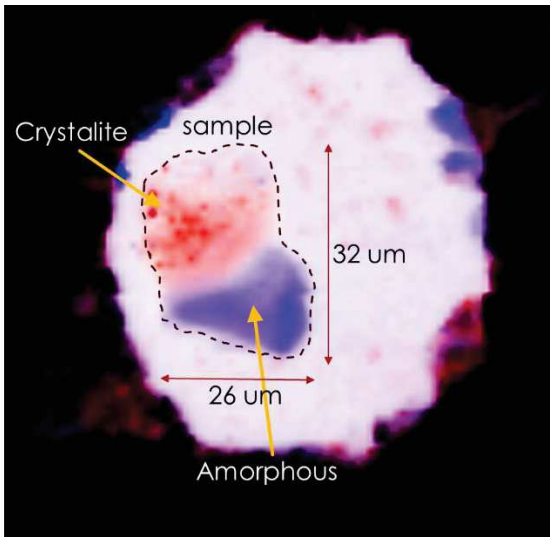

Fig. 4 Mapping of phase distribution by synchrotron radiation after heating of Mg glasses to 2750 K at 50 GPa and cooling to RT.

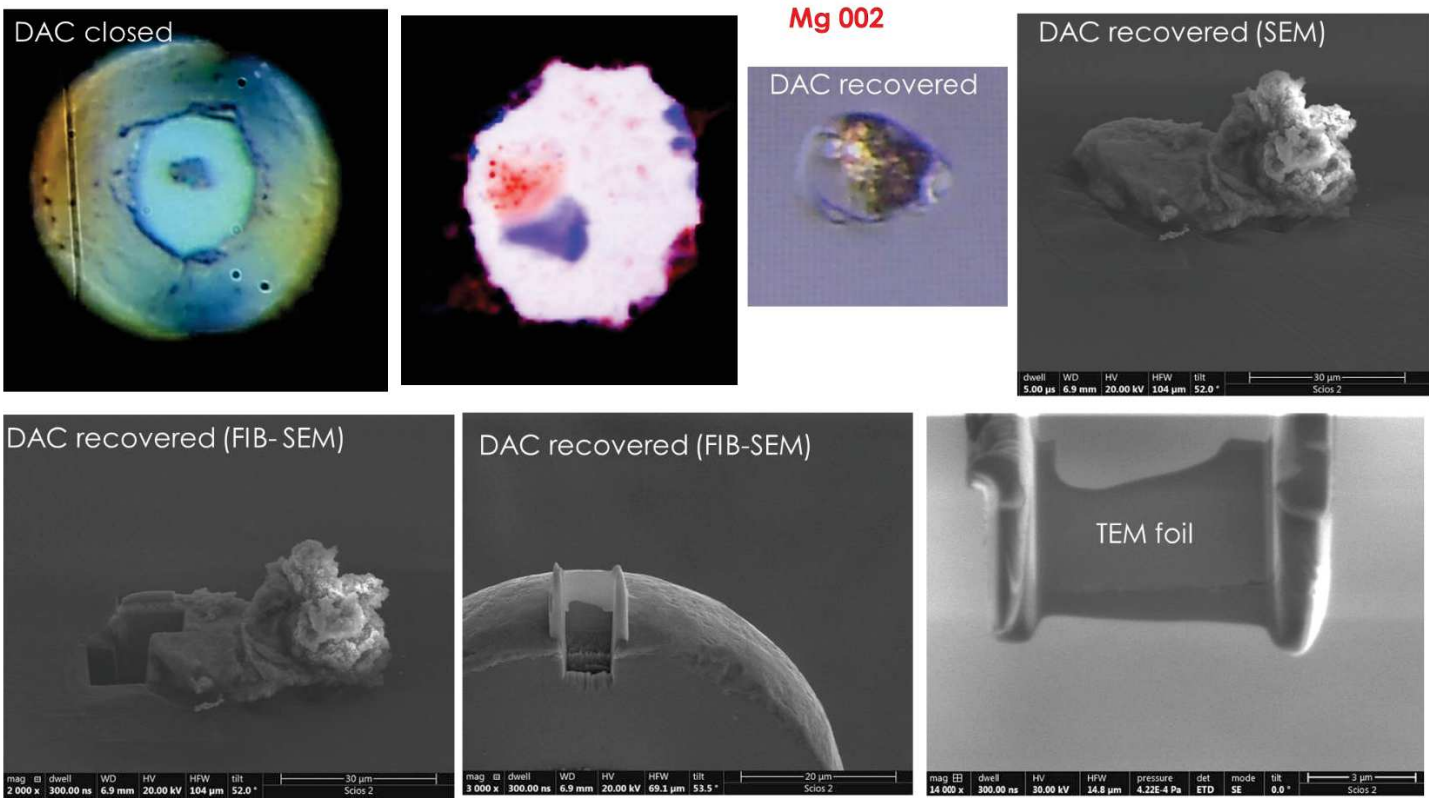

Fig. 5 DAC sample **$Mg_{61}Cu_{28}Gd_{11}$ %at.** recovered from 2750 K and 50 GPa ambient conditions characterization procedure (SEM observation, Focussed Ion Beam thin foil preparation).

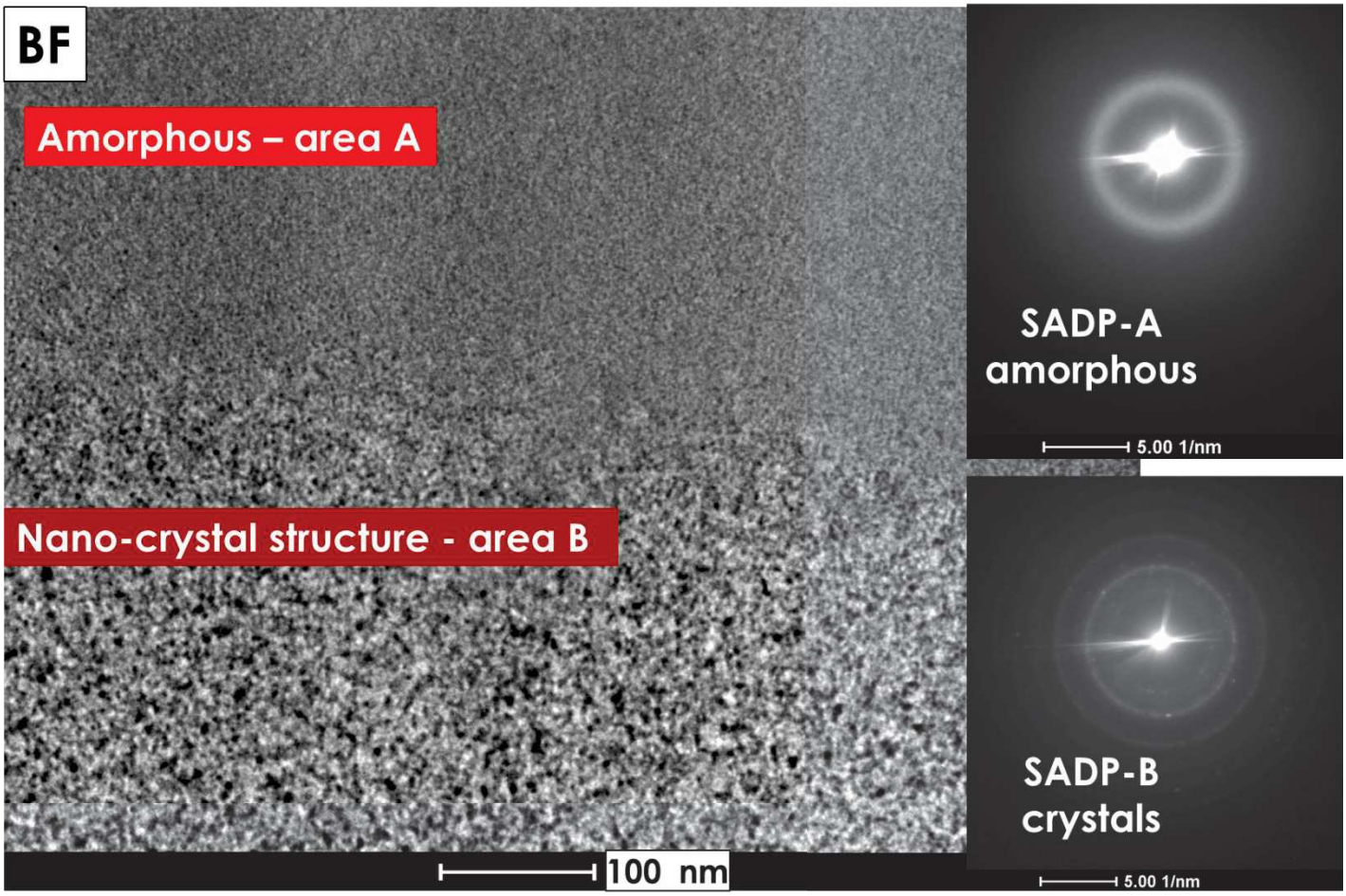

Fig. 6 Bright field image taken from area of amorphous (area A) / crystals (area B) sample with selected area diffraction patterns confirming the presence of fully amorphous (upper) and nanocrystalline (bottom) phases.

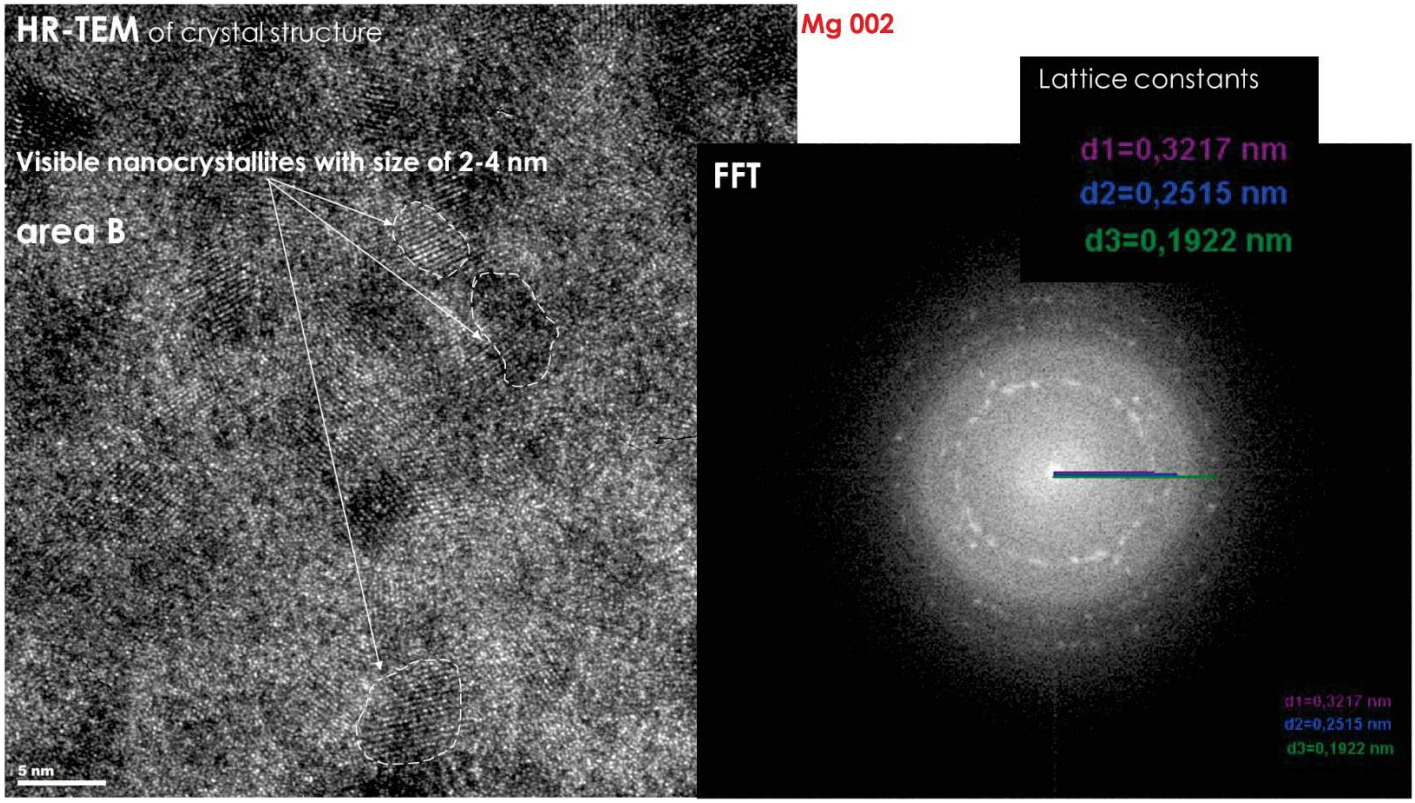

Fig. 7 High-resolution transmission electron image with inverse fast furrier transform.

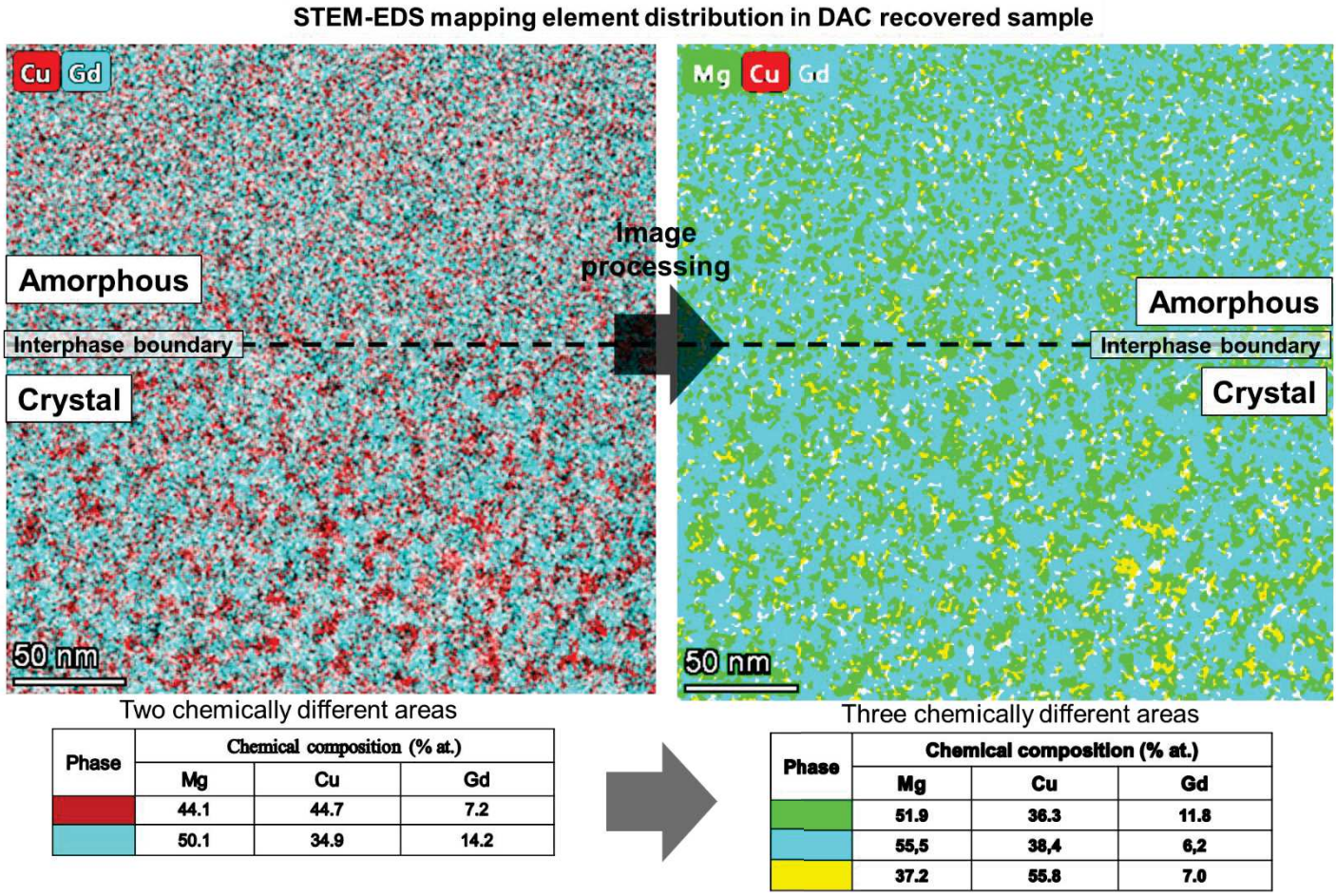

Phase	Chemical composition (% at.)		
	Mg	Cu	Gd
	44.1	44.7	7.2
	50.1	34.9	14.2

Phase	Chemical composition (% at.)		
	Mg	Cu	Gd
	51.9	36.3	11.8
	55,5	38,4	6,2
	37.2	55.8	7.0

Fig. 7 STEM-EDS maps of the Mg-based glass DAC recovered sample with marked individual distribution of Mg, Cu, and Gd elements (left side), processed digital image with precise chemical points analysis (right side).

Transmission electron microscopy (TEM) in bright field mode (BF) was used to investigate the microstructural evolution after the crystallization of MgCuGd metallic glass at 50 GPa and 2700 K. TEM observation (Fig. 6) revealed an amorphous region (Area A) transitioning into crystalline (Area B). This amorphous/crystalline interphase boundary is visible through changes in contrast within the TEM images and was further confirmed by selected area diffraction (SAD) patterns (Fig. 6, inserted). The amorphous area displayed a characteristic diffuse halo ring pattern (upper), while the crystalline regions exhibited diffraction spots arranged in concentric rings, indicative of nanocrystalline domains (bottom).

A high-resolution TEM (HRTEM) micrograph (Fig. 7), taken at a magnification of 560,000x, clearly showed ordered atomic planes, confirming the presence of nanocrystallites with sizes ranging from 2 to 5 nm. These nanocrystallites, exhibiting various orientations, suggest that the crystallization process occurred in a heterogeneous manner, with localized nucleation sites leading to the formation of crystalline clusters within the matrix.

High-angle annular dark-field (HAADF) imaging (Fig. 7) was also applied to investigate the interphase areas between the amorphous and crystalline regions. This technique identified nano-domains containing elements from the Mg, Cu, and Gd groups within the amorphous phase. Furthermore, within the crystallized structure, three distinct compositional regions were identified: (i) Mg-enriched, (ii) Cu-enriched, and (iii) Gd-enriched zones. These regions, varying in size and distribution, indicate early-stage phase separation, where clusters of specific elemental compositions formed during the initial stages of crystallization (above the glass transition temperature, *Tx*).

The results suggest that the crystallization process at ultra-high pressure and temperature initiated the segregation of elemental clusters, leading to the nucleation of nanocrystals. These nanocrystallites, composed primarily of Mg, Cu, and Gd-rich domains, represent the early phases of crystallization, which are further stabilized by the applied high pressure, promoting phase formation distinct from those observed at ambient conditions.

II Zr43Cu43Al7Ag7 %at glass

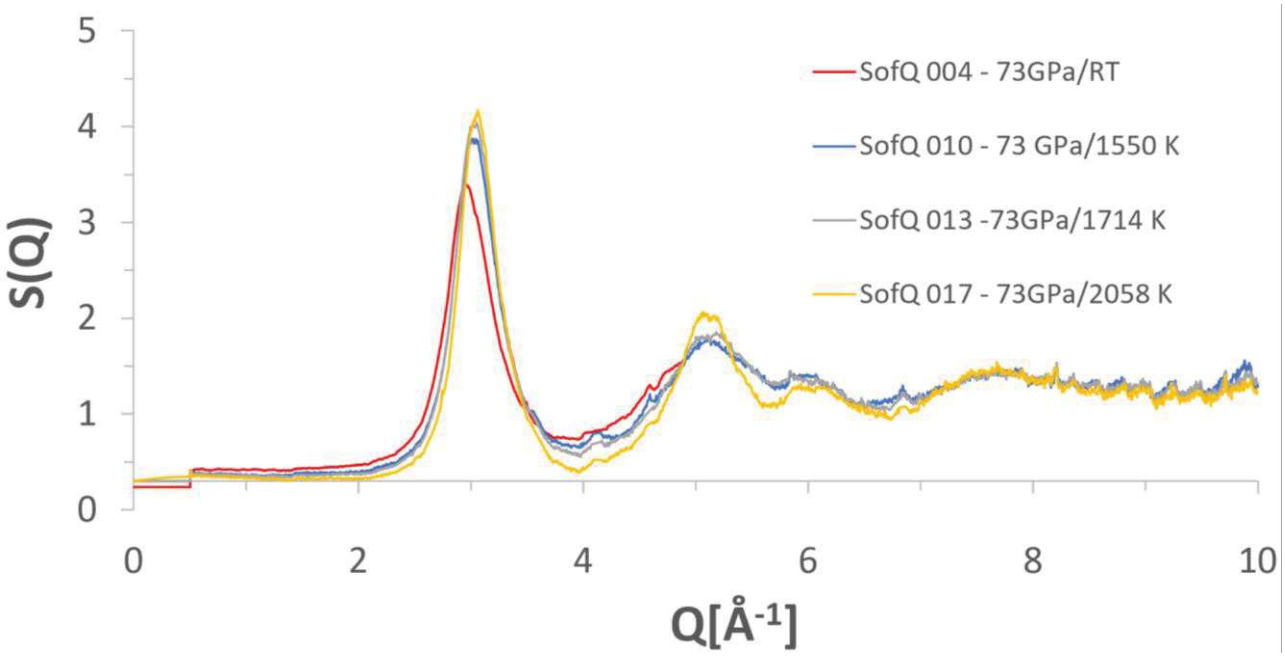

Fig. 8 Structure-function of selected $Zr_{43}Cu_{43}Al_7Ag_7$ %at. glasses.

Figure 4 shows example structure functions for $Zr_{43}Cu_{43}Al_7Ag_7$ %at. after quenching, under pressure, from different temperatures, e.g., 1550 K, 1714 K, 2058 K, and 2187 K. As a starting state for RT- materials, it was amorphous. For the alloy **$Zr_{43}Cu_{43}Al_7Ag_7$ %at. under a pressure of 73 GPa, the analysis of S(Q) and Q(Å^{-1}) data suggests significant structural changes as the quenching** temperature increases.

Room Temperature (73 GPa): S(Q) = 3.42, Q ≈ 2.96 Å^{-1}.
At room temperature and **73 GPa**, the structure is assumed to be **amorphous**. The relatively low value of **S(Q)** indicates a lack of long-range atomic order, which is typical for amorphous metallic glasses. The peak in **Q** reflects the characteristic short-range atomic packing, but no well-defined crystalline periodicity exists. Amorphous Zr-based alloys, such as ZrCuAl systems, typically exhibit broad, low-intensity peaks in **S(Q)**, consistent with disordered atomic arrangements.
Heated to 1550 K (73 GPa): S(Q) = 3.89, Q ≈ 3.02 Å^{-1}.
As the temperature is raised to 1550 K, S(Q) increases, suggesting the onset of nano-crystallization in the amorphous matrix. The shift in Q to higher values indicates a reduction in interatomic distances as the material begins to order. The increase in S(Q) reflects the growing degree of atomic order, suggesting that some regions of the alloy are starting to crystallize. However, the structure is not fully crystalline yet.
Heated to 1714 K (73 GPa): S(Q) = 4.05, Q ≈ 3.02 Å^{-1}.
At 1714 K, the further increase in S(Q) indicates that nano-crystallization in amorphous matrix is progressing, with more of the structure becoming ordered. The fact that Q remains relatively stable suggests that the atomic packing distances are not changing significantly, but the increased S(Q) indicates that more atoms are settling into a regular crystalline arrangement.
Heated to 2058 K (73 GPa): S(Q) = 4.195, Q ≈ 3.07 Å^{-1}.
At 2058 K, S(Q) reaches its highest value, indicating that the material has likely reached a fully crystalline state. The slight shift in Q to higher values suggests that the atomic distances have decreased slightly due to thermal expansion, but overall, the structure is highly ordered. The sharp increase in S(Q) confirms that a significant degree of long-range order has developed, consistent with a crystalline phase.

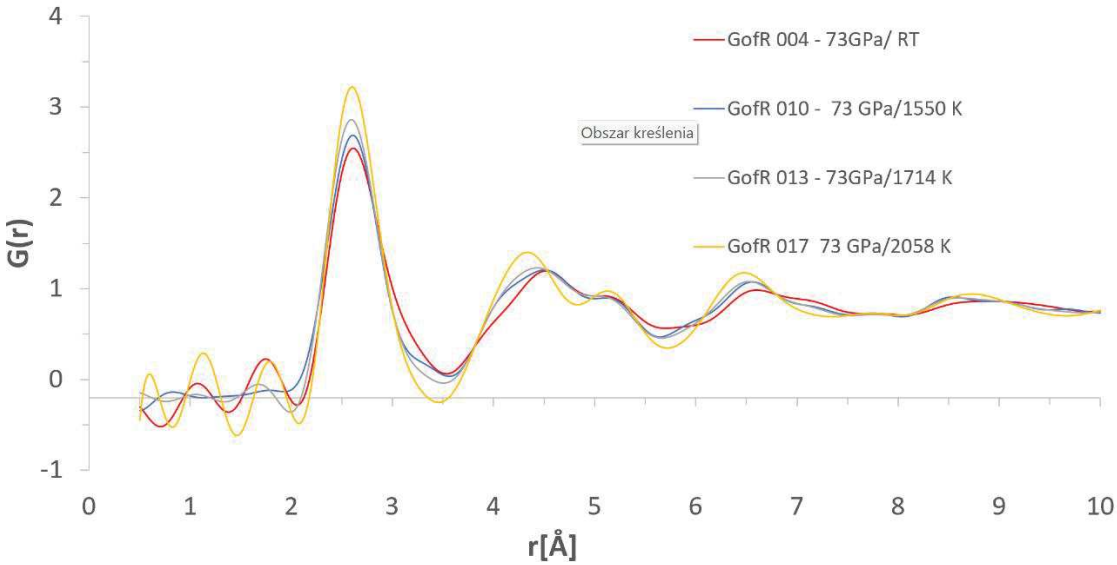

Fig. 9. Reduced pair distribution function corresponding to S(Q) samples (Zr43Cu43Al7Ag7 %at) shown in Fig. 8.

At **room temperature**, the **G(r) = 2.73**, with **r ≈ 2.59 Å⁻¹**, indicating a disordered, amorphous structure. In amorphous materials, the pair distribution function shows a broad first peak, which reflects short-range order due to nearest-neighbor atomic interactions but lacks long-range crystallinity. The high pressure (73 GPa) compresses the structure, reducing the average interatomic distances reflected in the r-value.
At **1550 K**, **G(r) increases to 2.92**, with **r ≈ 2.61 Å⁻¹**. This slight G(r) increase indicates that the material is undergoing partial crystallization. The slight shift in r suggests that while atomic distances have slightly expanded due to thermal effects, the overall structure remains constrained by the high pressure. The G(r) rise indicates that some local atomic ordering has occurred.
At **1714 K**, **G(r)** increases to **3.03**, with **r stabilizing at 2.59 Å⁻¹**. This suggests that crystallization has progressed, and more ordered regions are forming. The stable value of r implies that the average interatomic distances remain relatively constant, constrained by the high pressure. Still, the increasing G(r) reflects the growing degree of atomic order.
At **2058 K**, **G(r)** reaches **3.39**, with **r ≈ 2.60 Å⁻¹**. This significant G(r) increase indicates that the structure has likely achieved a high degree of crystallinity. The slight shift in **r** suggests that some thermal expansion occurs, but the overall structure remains under the influence of high pressure, keeping atomic distances relatively short.

Summary:
In the case of Mg- and Zr-based metallic glasses, high-pressure and high-temperature experiments revealed significant structural changes during heating, as seen in both S(Q) and G(r) functions. For Mg-based glass (MgCuGd), crystallization occurred at 50 GPa and 1500 K, with the S(Q) indicating shifts to higher Q values and increased amplitude, suggesting a transition from an amorphous state to a more ordered nanocrystalline structure. TEM confirmed the presence of nanocrystallites (2-5 nm) within the amorphous matrix, composed of Mg, Cu, and Gd-rich regions, marking the early stages of nano-crystallization.
Similarly, increased temperatures for Zr-based metallic glasses (ZrCuAlAg) led to structural ordering, with shifts in G(r) indicating decreasing atomic distances and increasing crystallinity. TEM analysis also revealed nanoscale crystallites and elemental segregation, further supporting the notion of temperature-driven crystallization starting from an initially amorphous state.
Both systems exhibited early-stage phase separation and crystallization under extreme conditions, with TEM providing crucial insight into the nanoscale structural evolution.